Journal Pre-proofs

Customizable orodispersible films: Inkjet printing and data matrix encoding for personalized hydrocortisone dosing

Lucía Rodríguez-Pombo, Paola Carou-Senra, Erea Rodríguez-Martínez, Patricija Januskaite, Carlos Rial, Paulo Félix, Carmen Alvarez-Lorenzo, Abdul W. Basit, Alvaro Goyanes

PII: S0378-5173(24)00239-4
DOI: https://doi.org/10.1016/j.ijpharm.2024.124005
Reference: IJP 124005

To appear in: *International Journal of Pharmaceutics*

Received Date: 2 February 2024
Revised Date: 8 March 2024
Accepted Date: 14 March 2024

Please cite this article as: L. Rodríguez-Pombo, P. Carou-Senra, E. Rodríguez-Martínez, P. Januskaite, C. Rial, P. Félix, C. Alvarez-Lorenzo, A.W. Basit, A. Goyanes, Customizable orodispersible films: Inkjet printing and data matrix encoding for personalized hydrocortisone dosing, *International Journal of Pharmaceutics* (2024), doi: https://doi.org/10.1016/j.ijpharm.2024.124005

Customizable orodispersible films: Inkjet printing and data matrix encoding for personalized hydrocortisone dosing

Lucía Rodríguez-Pombo[1], Paola Carou-Senra[1], Erea Rodríguez-Martínez[1], Patricija Januskaite[2], Carlos Rial[3,4], Paulo Félix[5], Carmen Alvarez-Lorenzo[1], Abdul W. Basit[2,3,4], Alvaro Goyanes[1,2,3,4]**

[1] Departamento de Farmacología, Farmacia y Tecnología Farmacéutica, I+D Farma (GI-1645), Facultad de Farmacia, Instituto de Materiales (iMATUS) and Health Research Institute of Santiago de Compostela (IDIS), Universidade de Santiago de Compostela, 15782 Santiago de Compostela, Spain.

[2] Department of Pharmaceutics, UCL School of Pharmacy, University College London, 29-39 Brunswick Square, London, WC1N 1AX, UK.

[3] FABRX Ltd., Henwood House, Henwood, Ashford, Kent, TN24 8DH, UK.

[4] FABRX Artificial Intelligence, Carretera de Escairón, 14, Currelos (O Saviñao) CP 27543, Spain.

[5] CiTIUS, Universidade de Santiago de Compostela, 15782, Santiago de Compostela, Spain.

* Correspondence: a.basit@ucl.ac.uk (A.W.B.); a.goyanes@fabrx.co.uk (A.G.)

Abstract

The aim of this study was to exploit the versatility of inkjet printing to develop flexible doses of drug-loaded orodispersible films that encoded information in a data matrix pattern, and to introduce a specialised data matrix-generator software specifically focused on the healthcare sector. Pharma-inks (drug-loaded inks) containing hydrocortisone (HC) were developed and characterised based on their rheological properties and drug content. Different strategies were investigated to improve HC solubility: formation of β-cyclodextrin complexes, Soluplus® based micelles, and the use of co-solvent systems. The software automatically adapted the data matrix size and identified the number of layers for printing. HC content deposited in each film layer was measured, and it was found that the proportion of co-solvent used directly affected the drug solubility and simultaneously played a role in the modification of the viscosity and surface tension of the inks. The formation of β-cyclodextrin complexes improved the drug quantity deposited in each layer. On the contrary, micelle-based inks were not suitable for printing. Orodispersible films containing flexible and low doses of personalised HC were successfully prepared, and the development of a code generator software oriented to medical use provided an additional, innovative, and revolutionary advantage to personalised medicine safety and accessibility.

Keywords: Desktop inkjet printing, 2D printed drug products, hydrocortisone, data-enriched edible pharmaceuticals, personalized medicine

1. Introduction

Conventional therapies follow a “one size fits all” approach, producing medicines with fixed doses for the entire population. While suitable for many, this approach poses challenges for drugs with a narrow therapeutic index(Wening and Breitkreutz, 2011) or highly variable pharmacokinetic and/or pharmacodynamic profiles(Edinger et al., 2018)(Vuddanda et al., 2018)(El-Maouche et al., 2017)(Abdel Jalil et al., 2021). The same strength administered to several patients may cause varied pharmacological responses due to interindividual factors, leading to under or over-dosing(Turner et al., 2015). Such undesirable therapeutic outcomes are more notable in the paediatric population because of the lack of child-appropriate formulations. It is common practice to modify dosage forms designed for adults before

administering to children, by preparing a suitable unlicensed medicine or by manipulating dosage forms at the point-of-care(Khan et al., 2022).

Hydrocortisone (HC) is the recommended glucocorticoid for treating adrenal insufficiency in childhood and puberty (deficiency of cortisol)(Nisticò et al., 2022). Cortisol production follows a circadian rhythm(Mohd Azmi et al., 2021), peaking in the morning and gradually decreasing throughout the day, reaching minimal levels at midnight. It is vital for patients to mimic this physiological pattern of cortisol production in their hormone replacement therapy to avoid decompensations(Chan and Debono, 2010) such as metabolic disorders, bone or weight loss, and cardiovascular disorders(Husebye et al., 2021). However, the replication of this pattern faces challenges due to the lack of versatility in the current manufacturing technologies. In clinical practice, the appropriate HC dose (8 - 10 mg/m^2/day) is calculated based on the body surface area and is administered between 2 - 4 times a day(El-Maouche et al., 2017).

Up to now, hydrocortisone medicines specific to the paediatric population are scarce. While Plenadren® modified-release tablets are approved by the European Medicines Agency (EMA) in certain doses, safety and efficacy data for paediatric use is still limited("Plenadren Product information. European Medicines Agency (EMA)," n.d.). Hydrocortisone modified-release capsules containing doses of 5, 10, or 20 mg (Efmody®) are approved by the EMA but are only indicated for adolescents > 12 years old and adults("Efmody Product information. European Medicines Agency (EMA), 2023.," n.d.). The recent Food and Drug Administration (FDA) and EMA approval of Alkindi® marks the first paediatric medicine for this disorder (birth to <18 years), available in capsules with hydrocortisone granules ranging from 0.5 mg to 5 mg("Alkindi Product information. European Medicines Agency (EMA), 2023.," n.d.). However, availability issues exist in certain European countries like Spain due to observed side effects when discontinuing conventional hydrocortisone treatment("Alkindi Product information. European Medicines Agency (EMA), 2023.," n.d.). As a result, HC formulations containing the specific dose are prepared manually at the dispensing point, and marketed tablets are crushed or HC suspensions are made in hospital pharmacies to comply with specific patient needs(Whitaker et al., 2015). However, pharmaceutical compounding is time consuming, resource-intensive, prone to dosing errors, and is an inflexible approach to meet continuous dose changes(Watson et al., 2021).

In the last decade, various additive manufacturing technologies have been explored to ensure a more personalized patient treatment approach(Cui et al., 2021; Daly et al., 2015; Nadagouda et al., 2020; Seoane-Viaño et al., 2021; Vaz and Kumar, 2021). Inkjet printing is gaining attention in the development of tailored oral dosage forms (Boehm et al., 2014; Carou-Senra et al., 2023; Chou et al., 2021; Kiefer et al., 2021; Öblom et al., 2020; Sandler et al., 2011). Traditional desktop inkjet printers have been successfully adapted to print a vast number of drugs such as caffeine and indomethacin on different substrates(Alomari et al., 2018; Arshad et al., 2020; Genina et al., 2013, 2012; Kiefer et al., 2021; Wickström et al., 2015). This material jetting technology involves the deposition of a controlled droplet pattern of pharma-ink (drug-loaded ink) on a substrate(Daly et al., 2015; Singh et al., 2010). This technology can be classified according to the mechanism of droplet generation. Thermal inkjet printing uses micro-resistors in direct contact with the ink, rapidly heating up to form a vaporization-induced bubble that expands, ejecting fluid through the nozzle to create a droplet(Meléndez et al., 2008). In piezoelectric inkjet printing, each nozzle is surrounded by a piezoelectric element that, when subjected to an electrical current, mechanically deforms the ink, generating pressure waves that expel droplets through the nozzle(Azizi Machekposhti et al., 2019). Inkjet printing has demonstrated success in various dosage forms, such as orodispersible or bioadhesive

films(Kiefer et al., 2021; Varan et al., 2017; Vuddanda et al., 2018), transdermal microneedles(Boehm et al., 2013), contact lenses(Pollard et al., 2023), drug-loaded stents(Scoutaris et al., 2016) and even direct application onto nails(Pollard et al., 2022).

The versatility and precision of inkjet printing technology allows the design of unique digital patterns on substrates, introducing novel dosage forms (data-enriched edible pharmaceuticals - DEEPs), with information easily readable by smartphones (Chao et al., 2022, 2021; Edinger et al., 2018; Öblom et al., 2020). oThe required dose is printed as a QR or data matrix code, providing encoded information such as drug name, dose, patient details, prescribing instructions, side effects, expiry date, manufacturer identification and the batch number to patients and/or healthcare professionals(Handa et al., 2023). The use of QR codes and smart devices has demonstrated improvements in tracking, safety, and adherence to prescribed dosage schedules, leading to reduced visits to health professionals(Chao et al., 2021; Edinger et al., 2018). Although studies have explored QR code printing on films using free online QR generators, the development of healthcare-specific software remains unexplored(Chao et al., 2021; Edinger et al., 2018). A specialised software would ensure the tracking and traceability of the drug product directly to the patient, presenting a significant opportunity to utilize inkjet printing to prepare data-enriched dosage forms, improving treatment safety and efficacy(Nørfeldt et al., 2019; Raijada et al., 2021).

The aim of this study was to evaluate the combination of inkjet printing and a data matrix code generator software specifically made for the healthcare sector, to produce data matrix films loaded with HC as the model drug. Various HC-loaded inks, incorporating different excipients, were developed to optimize inkjet printing performance. Inclusion complexes and micelle formation were evaluated to improve poor drug solubility within the pharma-ink, since they are available pharmaceutical strategies to overcome solubility issues of poorly water-soluble drugs (Rodriguez-Aller et al., 2015). The pharma-inks were printed on edible substrates using conventional desktop printers, following a data matrix pattern generated by the developed software. The study varied the number of printed layers and data matrix size to achieve personalized doses, quantifying the total HC printed in different layers.

2. Materials and Methods

2.1 Materials

Hydrocortisone base (MW 362.46 g/mol, Acofarma, Barcelona, Spain); 1,2-propylene glycol (Scharlau, Barcelona, Spain); MilliQ® water; Methanol (Merck, Darmstadt, Germany); Ethanol (VWR International, Radnor, USA); E-122 Red colorant (Guinama, Valencia, Spain); Bright blue colorant (Guinama, Valencia, Spain); β-Cyclodextrin (β-CD; Nihon Shokuhin Kako Co. Ltd, Tokyo, Japan); Soluplus® (polyvinyl caprolactam polyvinyl acetate-polyethylene glycol grafted copolymer, BASF, Ludwigshafen, Germany); SensiJet® (Sensient, Milwaukee, USA); Potato starch edible paper (0.3 mm thickness; Decoración Dulce, Madrid, Spain); Rice edible paper (0.4 mm thickness; Decoración Dulce, Madrid, Spain).

2.2 Pharma-ink formulation

Several placebo inks (no drug) with different solvent ratios were prepared (Table S1). Pharma-inks containing HC were also prepared by dissolving 300 mg of HC in 25mL of varying ratios of 1,2-propylene glycol (PG) and water as shown in Table 1. The formation of HC:β-CD inclusion complexes and the formation of micelles with Soluplus® were tested to increase the poor drug solubility and the amount of deposited drug in each printed layer.

β-CD was added in different weight ratios for the formation of the inclusion complexes with the drug; namely HC:β-CD 1:3 and 1:6 w/w, which corresponded to 1:1 and 1:2 mol ratio. The same amount of HC (300 mg) and the corresponding amount of β-CD in each of the cases (900 mg and 1800 mg of β-CD respectively) were placed in a flask. 25 mL of propylene glycol:water (PG:H_2O) mixture was added and incubated at 37 °C for 24 h, in a shaker at 100 rpm. Approximately 4 mg of E-122 red colorant was added to PG:H_2O (30:70 v/v) and E-133 blue colorant to PG:H_2O (60:40 v/v). The final solution was filtered through a 0.45 μm filter.

Soluplus 6% (w/w) and 10% (w/w) were used for the formation of micelles. The corresponding quantity of Soluplus and 300 mg of HC were added into a flask. 25 mL (Soluplus at 6% w/w) and 35 mL (Soluplus at 10% w/w) were added and incubated for 24 h at 37 °C in a shaker at 100 rpm. The addition of the E-133 blue colorant as well as the subsequent filtering of the formulation was carried out in the same method, as described earlier.

Table 1. Composition of developed pharma-inks. All formulations contained 300 mg of HC and 4 mg of colourant.

Pharma-ink	Water (v/v)	Propylene glycol (v/v)	Solubility modifier	Solubility modifier content (w/w)
PG:H_2O (30:70 v/v)+ HC	70	30	-	-
PG:H_2O (60:40 v/v)+ HC	40	60	-	-
PG:H_2O (30:70 v/v)+ HC:β-CD	70	30	HC: β-CD	1:3
PG:H_2O (60:40 v/v)+ HC:β-CD	40	60	HC: β-CD	1:3
PG:H_2O (30:70 v/v)+ HC:β-CD	70	30	HC: β-CD	1:6
PG:H_2O (60:40 v/v)+ HC:β-CD	40	60	HC: β-CD	1:6
PG:H_2O (30:70 v/v)+ HC:Soluplus	70	30	Soluplus	6
PG:H_2O (60:40 v/v)+ HC:Soluplus	40	60	Soluplus	6

PG:H_2O (30:70 v/v)+ HC:Soluplus	70	30	Soluplus	10
PG:H_2O (60:40 v/v)+ HC:Soluplus	40	60	Soluplus	10

2.3 Pharma-ink characterization

The inks were characterised based on their viscosity, surface tension, and density to evaluate their printability.

2.3.1 Dynamic viscosity

Viscosity was measured in duplicate (n=2) using a Rheolyst AR 1000-N Rheometer (TA Instruments, New Castle, DE, USA) equipped with a cone-plate geometry. Measurements were conducted with a cone (ø 60 mm, angle 2.1°) on the Peltier plate set up at 20 °C. Approximately 2 mL of the ink was transferred to the plate. The sample was subjected to a shear rate ramp from 0.05 to 1000 s^{-1} and the run time was 5 minutes. The upper limit of the shear rate ramp (1000 s^{-1}) was taken as the viscosity value of the ink.

2.3.2 Surface tension

Surface tension was determined in duplicate (n=2) following the platinum ring method using a Lauda Tensiometer TD1 (Lauda Scientific GmbH, Lauda-Königshofen, Germany) at room temperature and applying the needed corrections(Ebnesajjad S., 2009). The platinum ring with a well-defined geometry was submerged in the ink and the pull force was measured according to Equation 1:

$$P_T = P_R + 4\,\pi\,r\,\gamma_{ideal} \qquad (1)$$

Where P_T is the total force on the ring, P_R is the weight of the ring, r is the radius of the ring, and γ_{ideal} is the ideal surface tension. In practice, a meniscus correction factor was required as the size and shape of the surface inside and outside the ring are not the same. Surface tension was corrected for the shape of the ring by a factor (f) as shown in Equation 2:

$$\gamma = f\,\gamma_{ideal} \qquad (2)$$

2.3.3 Density

The density of each ink was measured with an ABT 220-4NM analytical balance (KERN & SOHN GmbH, Stuttgart, Germany). 1 mL of the ink was removed using a PIPETMAN L Fixed F1000L Gilson Pipette (accuracy (%/µL) 0.5/5.0, Gilson Inc., Middleton, WI, USA) and accurately weighed at 25 ºC. The average of three measurements was used as the density of the ink.

2.3.4 Nozzle diameter measurement

An Olympus CKX53 optical microscope (Tokyo, Japan) was used to observe the orifice diameter in the HP27 cartridge. The measurements were made using 4x and 10x magnifications with a scale in micrometres.

2.3.5 Z value determination

A printability prediction was made by calculating the *Z* value, a dimensionless equation which helps predict droplet behaviour based on the physical characteristics of the pharma-ink and nozzle specifications. The diameter of the printer nozzle (d, in µm), ink density (ρ, in g/mL), surface tension (σ, in mN/m), and viscosity (η, in mPa*s) were used for the calculation of the *Z* value according to the following Equation 3(Jang et al., 2009):

$$Z = \frac{\sqrt{\rho d \sigma}}{\eta} \qquad (3)$$

2.3.6 Solubility assay

Solubility was measured via saturation, adding the drug until no more dissolved, followed by analysis of the final drug concentration in each pharma-ink. A 0.5 mL aliquot of each prepared pharma-ink (25 mL) was taken and diluted in a 50 mL flask using methanol:water (50:50 v/v) with 1% formic acid as dilution medium. 2 mL of the sample was filtered using 0.22 µm filters (Millipore Ltd., Dublin, Ireland) and the drug concentration was determined using high performance liquid chromatography-ultraviolet (HPLC-UV) (JASCO LC-4000 Series, Jasco, Madrid, Spain), with the method described in another section. All measurements were performed in duplicate (n=2).

2.4 Data matrix code-generator software prototype

The data matrix code-generator M3DIMAKER Studio™ software (FABRX Ltd., London, UK) was designed specifically for medical use. Scaled data matrix codes were generated by filling a simple form (Figure 1A). Once the application form was filled and the printing confirmed, the software generated a PDF document with the scaled data matrix codes which encoded the information of interest. In addition, the number of printing layers necessary to obtain the target dose was indicated. For the size scalation of the data matrix, the software used parameters such as the printer resolution and the volume of ink that the printer deposits in each drop (often in picolitres). When the PDF was generated, ODFs could be obtained with drug doses adapted to the medical needs of each patient, with the software personalizing the required dose quickly and easily.

The healthcare professional would select the number of printed dosage forms based on the prescribing instructions for the patient. Up to 28 drug-loaded films containing encoded-information could be printed during a single print. A choice of single printing (Figure 1A) or multiple dose printing (Figure 1B) was available within the software. Single printing generated up to 28 data matrix codes containing the same dose; multiple printing generated data matrix codes with varying dose.

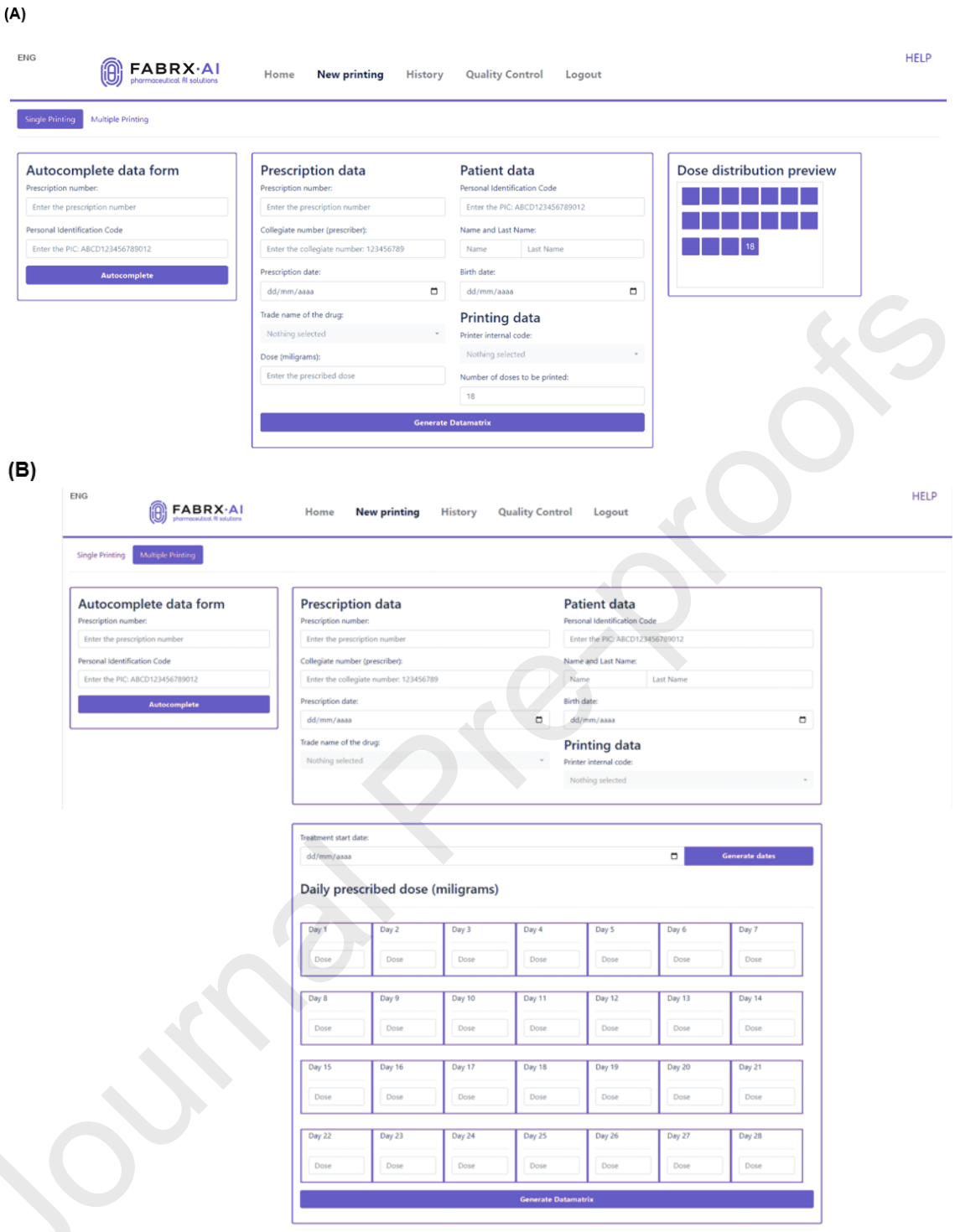

Figure 1. Data application forms within the software to be filled to obtain the PDF with the data matrix codes for (A) Single dose printing and (B) Multiple dose printing.

2.5 Inkjet printing of hydrocortisone films

The printing tests were carried out using two unmodified desktop printers: a thermal inkjet printer, HP Deskjet 3420 (Hewlett Packard, Palo Alto, USA) (Figure 2A), and a piezoelectric inkjet printer, Canon Pixma TS705 (Canon Inc., Tokyo, Japan) (Figure 2B).

HP printer ink cartridges (black and tri-colour, model numbers HP27 and HP28, respectively) and a Canon cartridge (PGI 580 black cartridge) were modified by cutting off the top, removing the sponges, and removing the commercial ink with distilled water, followed by ethanol. Once the cartridges were cleaned, they were loaded with the custom developed pharma-inks and placed inside the printer.

Figure 2. The printers (left) and opened cartridges (right): (A) HP Deskjet 3420 (HP 27 and HP 28), and (B) Canon Pixma TS705 (PGI 580 black cartridge) used in the study.

Printing tests were performed on two commercially available edible inert substrates: a substrate based on potato starch with a thickness of 0.3 mm and a substrate based on rice with a thickness of 0.4 mm were used in the study. Both substrates behave as orodispersible films (ODFs) allowing for the immediate release of the drug. ODFs are intended to be placed onto the tongue where they dissolve rapidly in the saliva(Hoffmann et al., 2011). This approach holds particular promise for the paediatric population as it eliminates the need for swallowing the entire dosage form, reducing the risk of choking and enhancing overall patient acceptability.

In both cases, the deposition of the pharma-ink considerably moistened the substrate; therefore, between prints, it was necessary to leave the substrate for 10 min at room temperature before printing the next layer. Ideally, the substrate would absorb the pharma-ink faster to reduce the drying process time between the printed layers. Considering that the films used were prefabricated and for which characteristics have already been established, no further characterization of the substrates was carried out.

2.6 Drug content in the printed films

The samples of the different printed films were placed in a volumetric flask (25 ml) with methanol and Milli-Q® water (50:50 v/v) with 1% v/v formic acid with magnetic stirring until complete extraction of the drug (overnight). Sample solutions were then filtered through 0.22 µm filters (Millipore Ltd., Dublin, Ireland) and the concentration of drug was determined with HPLC-UV (JASCO LC-4000 Series, Jasco, Madrid, Spain). The assay entailed injecting 30 µL samples for analysis using a mobile phase of methanol and water (70:30 v/v) containing 1%

v/v formic acid through a Symmetry 5 µm C18 column, 4.6 mm x 250 mm column (Waters, Milford, Massachusetts) maintained at 30 °C. The mobile phase was pumped at a flow rate of 1 mL/min and the eluent was screened at a wavelength of 250 nm. All measurements were made in duplicate. The retention time was 4.1 minutes, and the concentration range was 0.07-160 µg/mL.

2.7 Disintegration testing

Disintegration time was analysed to study the mechanical break of the developed pharmaceutical form, using the slide frame method. For this purpose, the film (2 x 6 cm; width x length) was placed completely flat on top of a 50 mL beaker (4.5 cm diameter), completely covering the beaker so that it was under tension. 200 µl of simulated saliva (previously heated at 37°C) was added centrically on the film surface using a micropipette (the same pipette as described in Section 2.3.3). The time required for the simulated saliva to wet the film matrix until the first drop falls into the beaker was measured. Measurements were performed in quadruplicate (n = 4).

3. Results and discussion

3.1 Pharma-ink characterization

Inkjet printing performance is conditioned by the jetting capacity of the pharma-ink, therefore the rheological properties of the ink are limiting factors that need to be taken into account(Nallan et al., 2014). It is reported that the optimum viscosity range for inks in inkjet printing applications is between 1 - 25 mPa*s(Waasdorp et al., 2018). The viscosity values varied widely in the tested inks (Table 2). These differences could be attributed to the percentage of PG and the presence of solubility modifiers in the ink; both increasing the viscosity. According to Table 2, as the percentage of PG increased, so did the viscosity. When the solubility modifiers (inclusion complexation with β-CD and formation of micelles with Soluplus®) were added to the ink, the viscosity also increased.

The density values were similar for all tested pharma-inks. The addition of organic solvent and solubility modifiers (micelles and inclusion complexes) did not significantly affect this parameter. Typically, the optimum density range for adequate printing is 0.9 - 1.1 g/mL according to the literature(Waasdorp et al., 2018). The formulated inks had density values within the optimal range which indicated that the droplet formation process could be carried out (Table 2).

In terms of surface tension, the results obtained in the studied pharma-inks differed significantly (Table 2). According to the literature, the optimal surface tension range for the adequate formation of droplets is between 20-50 mN/m(Waasdorp et al., 2018). Considering that the surface tension of water has a value of 72 mN/m, inks with a large proportion of water are theoretically not printable. As the proportion of PG increased, the surface tension decreased because PG is a surfactant, exhibiting lower intermolecular forces with water molecules in comparison to water-water molecule interactions.

Table 2. Properties of the developed pharma-inks and printability results based on *Z* value. Data are shown as mean value ± SD. An experimental printability result of "-" designates a paper jam whereby printing could not be continued.

Pharma-ink	HC solubility (mg/mL)	Density (g/mL)	Surface tension (mN/m)	Viscosity (mPa*s)	*Z* value		Experimental printability (Y/N)	
					HP	Canon	HP	Canon
PG:H_2O 30:70 v/v + HC	1.10 ± 0.00	1.017 ± 0.007	46.6 ± 0.0	4.06 ± 0.54	7.6	5.1	Y	-
PG:H_2O 60:40 v/v +HC	5.84 ± 0.03	1.030 ± 0.001	36.7 ± 0.1	10.21 ± 0.28	2.7	1.8	Y	-
PG:H_2O 30:70 v/v + HC:*β*-CD (1:3 w/w)	2.40 ± 0.01	1.000 ± 0.005	46.6 ± 0.1	4.62 ± 1.17	6.6	4.4	Y	-
PG:H_2O 60:40 v/v + HC:*β*-CD (1:3 w/w)	6.74 ± 0.01	1.025 ± 0.002	36.8 ± 0.3	10.64 ± 0.37	2.6	1.7	Y	-
PG:H_2O 30:70 v/v + HC:*β*-CD (1:6 w/w)	3.01 ± 0.01	1.023 ± 0.003	44.5 ± 0.0	4.32 ± 0.75	7.0	4.7	Y	-
PG:H_2O 60:40 v/v + HC:*β*-	7.40 ± 0.01	1.051 ± 0.004	37.9 ± 0.2	11.25 ± 0.49	2.5	1.7	Y	-

CD (1:6 w/w)								
$PG:H_2O$ 30:70 v/v + HC+ Soluplus (6% w/w)	4.15 ± 0.04	1.024± 0.004	40.8 ± 0.0	7.99 ± 2.52	3.6	2.4	N	N
$PG:H_2O$ 60:40 v/v +HC+ Soluplus (6% w/w)	6.17 ± 0.04	1.036 ± 0.005	40.4 ± 0.3	35.65 ± 1.95	0.8	0.5	N	N
$PG:H_2O$ 30:70 v/v + HC+ Soluplus (10% w/w)	5.39 ± 0.03	0.995 ± 0.009	40.3 ± 0.1	21.55 ± 1.58	1.3	0.9	N	N
$PG:H_2O$ 60:40 v/v +HC + Soluplus (10% w/w)	10.66 ± 0.07	1.026 ± 0.004	38.0 ± 0.0	58.40 ± 0.29	0.5	0.3	N	N

The nozzle diameter of the HP27 cartridge was measured using an optical microscope and the diameter of the orifice was found to be 20 µm (Figure 3).

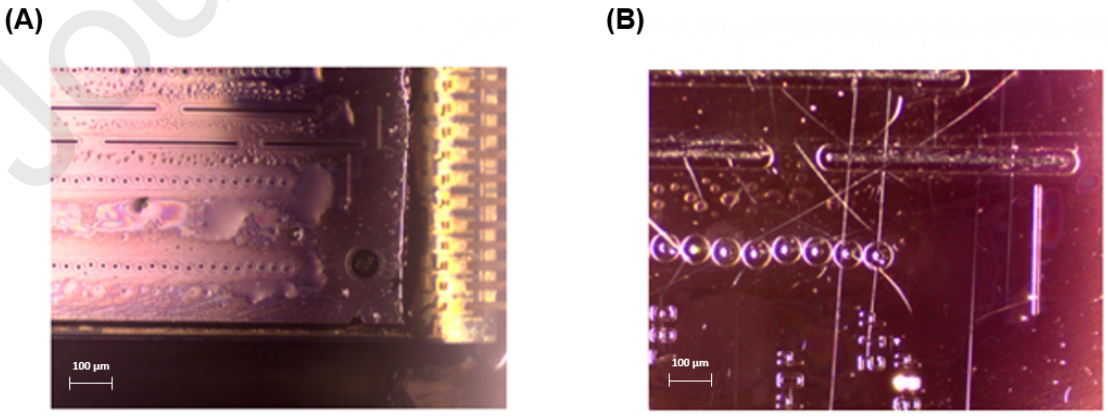

Figure 3. Pictures of the HP27 cartridge nozzles taken using an optical microscope for (A) 4x magnification, and (B) 10x magnification. Scale in µm.

According to the cartridge specifications, the nozzle diameter of the Canon cartridge is 9 µm, therefore, this value was used to calculate the Z value of the inks (Table 2 and 2S).

3.1.1 Printability determination using the Z value

Z values for all the developed pharma-inks were calculated as a printability prediction indicator (Tables 2 and 2S). Conventionally, the *Z* value (the reciprocal of the Ohnesorge number) is used in inkjet printing to predict if the ink will be jettable. If an ink has a *Z* value ranging between 1 - 10, it is often considered to be printable(Derby, 2015). However, it is reported that there are several exceptions in which *Z* values were above 10 and the inks were printable(Liu and Derby, 2019). Recently, machine learning (ML) algorithms to predict printability in inkjet printing applications were developed(Carou-Senra et al., 2023). Authors found in the exploratory data analysis on the *Z* values of extracted formulations that some inks (31.05% of printable formulations with known *Z* values) remained printable despite possessing a *Z* value of > 10. The findings of the mentioned study highlighted that printability depends on multiple factors and the printing results cannot be solely determined by the *Z* value of a formulation. The ML algorithm could not be used in this study due to the requirement of more datasets based on various factors. By training the developed ML models with more negative data, prediction performance could be improved, and this tool may be implemented in silico in the pharmaceutical field, accelerating the research and development of inkjet formulations.

Z values within the optimal range were obtained for most of the studied inks. Inks with higher viscosity values had a low *Z* value and were outside of the optimal established range, meaning that the formation of the drops was not optimized, but it does not imply that they cannot be used to carry out the printing process.

To investigate the feasibility of the Z value prediction, some pharma-inks were tested in both printers. A few inks could be printed with the Canon printer, but some could not due to the paper jamming inside the printer (referred to as "-" in Tables 2 and 2S). During printing in the Canon printer, the paper was placed at the bottom of the device and was guided to the top where the cartridges were located. During this movement, the paper must bend and withstand tension at the back of the printer, which allows it to move towards the printhead area. This phenomenon is related to the mechanical properties of the paper. Due to the tensile strength of the edible films, which are less flexible and differ from the commercially used A4 paper, this tension was sometimes not supported and resulted in the film breaking in two, jamming the printer. The paper jam was frequent in the Canon printer when printing the drug-loaded films but was avoided with the HP printer. As predicted by the Z value in Table 2, PG:H_2O 60:40 v/v + HC + Soluplus (6% w/w) and PG:H_2O 60:40 v/v + HC + Soluplus (10% w/w) inks were not printable (Table 2) because the Z value was outside the optimal range. However, some of the inks within the Z value range of 1 - 10 were also not printable. For instance, PG:H_2O 30:70 v/v + HC + Soluplus (6% w/w) (Table 2) had a Z value of 3.6 and 2.4 but was not printable in both printers. In addition, PG:EtOH 40:60 v/v ink (Table 2S) was also not printable although the Z value was in the accepted range. Ink printability can vary from one printer to another (HP vs Canon) as is seen in Table 2S. For example, PG:H_2O 60:40 v/v ink was only printable with the HP printer; the PG:H_2O 30:70 v/v ink rendered low quality prints with the Canon printer; the PG:EtOH 30:70 v/v ink was only printable with the Canon printer although the Z value was between the optimal range for both printers (Table 2S). Such variations could be explained by the fact that inkjet printing depends on a wide variety of parameters, some of them inherent to

each printer, such as the cartridge nozzle diameter or the droplet ejection mechanism (thermal vs piezoelectric). According to the results, it is important to highlight that the Z value is not the sole predictor of inkjet printability, and that other factors should be considered during ink development.

In view of the results obtained from the trial-and-error tests displayed in Tables 2 and 2S, and the frequent edible paper jamming in the Canon printer, the printer that provided the most versatility (more printable inks) and less variability in the printing process with the edible paper was the HP Deskjet 3420 and, for this reason, it was the selected printer to carry out the printing tests.

3.1.2 Solubility test

As the proportion of organic component (PG) increased, so did the solubility of HC as it is more soluble in PG compared to water (Figure 4)("Hydrocortisone | C21H30O5 | CID 5754 - PubChem," n.d.). In the case of the ink with a lower proportion of PG (PG:H_2O 30:70 v/v), a HC concentration of 1.10 mg/mL was obtained, whilst in the ink with a higher proportion of PG (PG:H_2O 60:40 v/v), a HC concentration of 5.8 mg/mL was obtained (Table 2).

As the concentration of HC in both inks may not be high enough to print the desired doses, the possibility of increasing the solubility using β-CD inclusion complexes and Soluplus® micelles was investigated. In both cases, the solubility of HC increased (Table 2). The improvement was more notable in the pharma-inks with a lower PG proportion. Solubility tests were performed with inclusion complexes at two different HC:β-CD mass ratios, 1:3 w/w (molar ratio 1:1) and 1:6 w/w (molar ratio 1:2), at different incubation times (1 day or 7 days). According to Table 2, a larger cyclodextrin amount (1:6 w/w) led to a greater solubility improvement in comparison to 1:3 w/w and no cyclodextrin, for both 60:40 v/v and 30:70 v/v HC:β-CD. However, the total amount of HC in 25mL of the pharma-inks containing β-CD was 145.75 mg, 168.5 mg and 185 mg for PG:H_2O 60:40 v/v, 1:3 w/w and 1:6 w/w HC:β-CD complex pharma-inks, respectively. The total amount of HC quantified in 25 mL was 27.5 mg, 60 mg and 75.25 mg for PG:H_2O 30:70 v/v, 1:3 w/w and 1:6 w/w HC:β-CD complexes, respectively. Therefore, the initial amount of HC (300 mg) added to the ink was not all encapsulated and was lower compared to the PG:H_2O 60:40 v/v pharma-ink. This total amount of HC is referred to as the combination of both free HC (not complexed with β-CD) and complexed HC. The methanol used as the mobile phase in HPLC analysis broke the formed HC:β-CD complexes so the total amount of HC in the pharma-inks (hydrocortisone dissolved in the pharma-ink and complexed hydrocortisone) was successfully quantified using the original HPLC method described in Section 2.6.

Despite a greater cyclodextrin ratio resulting in slightly higher solubility, the improvement obtained was not high enough considering the resource consumption to produce the 1:6 w/w HC:β-CD complex. Therefore, the ink containing HC:β-CD (1:6 w/w) was discarded. The solubility of HC at different incubation times was also studied using the same ratio of HC:β-CD. The solubility was slightly higher with longer incubation time (9.85 mg/mL for 7 days of incubation vs 6.74 mg/mL for 1 day of incubation). In view of the results, it can be stated that, for the times studied, 1 and 7 days, it was more efficient to use shorter incubation times since the main objective was to prepare on-demand films.

Another strategy to increase HC solubility was the formation of micelles using Soluplus®. An improvement in solubility was obtained, but ink properties were not suitable for inkjet printing (Table 2). The ink was not deposited on the substrate, and it was not possible to print a successful film.

Ink solubility with a higher proportion of PG was also studied but substituting water for ethanol. When ethanol was used instead of water, the drug solubility increased significantly and reached a HC concentration of 20.1 mg/mL because HC has a higher solubility in ethanol("Hydrocortisone | C21H30O5 | CID 5754 - PubChem," n.d.). However, PG:EtOH 60:40 v/v ink was not printable with the HP desktop printer (Table 2S). Although PG:EtOH 60:40 v/v ink showed the highest drug solubility, it could not be used due to the inconsistency in the printing process with the Canon printer also (paper jam and damage).

3.2 Data matrix code-generator software prototype

The developed software generated two PDF documents from the information filled in the application: a daily calendar (Figure 4A) and a document with the scaled data matrix codes (Figure 4B).

(A)

15 Nov - Tuesday	16 Nov - Wednesday	17 Nov - Thursday	18 Nov - Friday	19 Nov - Saturday	20 Nov - Sunday	21 Nov - Monday
22 Nov - Tuesday	23 Nov - Wednesday	24 Nov - Thursday	25 Nov - Friday	26 Nov - Saturday	27 Nov - Sunday	28 Nov - Monday
29 Nov - Tuesday	30 Nov - Wednesday	01 Dec - Thursday	02 Dec - Friday	03 Dec - Saturday	04 Dec - Sunday	05 Dec - Monday
06 Dec - Tuesday	07 Dec - Wednesday	08 Dec - Thursday	09 Dec - Friday	10 Dec - Saturday	11 Dec - Sunday	12 Dec - Monday

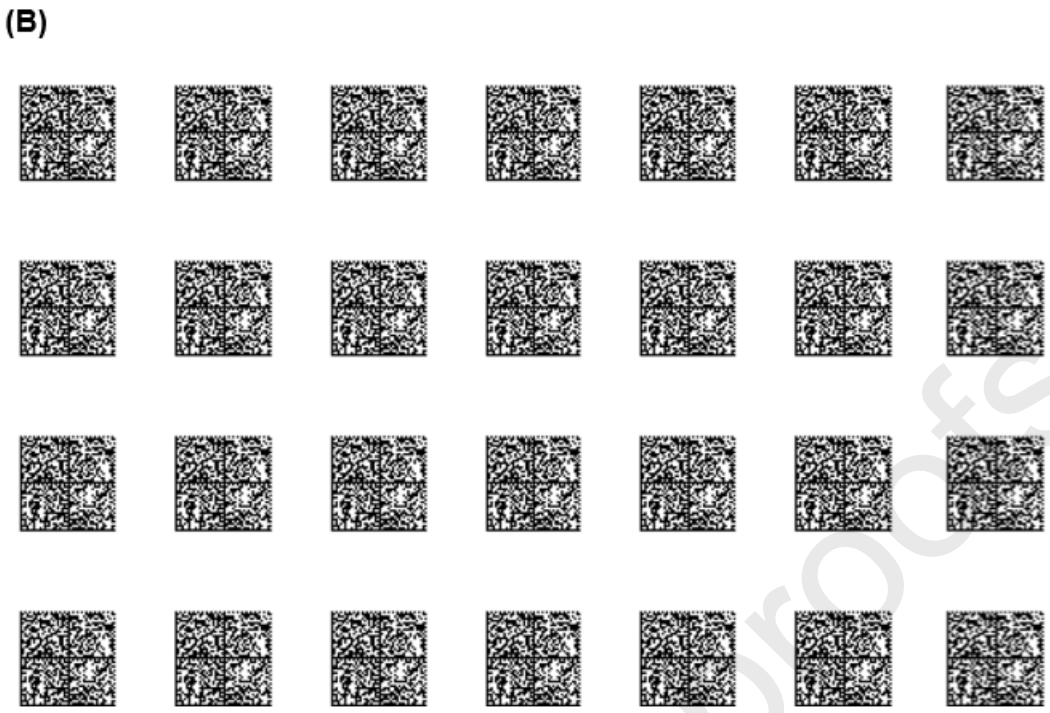

Figure 4. Images of the PDF documents generated with the M3DIMAKER Studio™ software: (A) A daily calendar that would be printed onto an edible substrate with the commercial SensiJet® ink and (B) Data matrix codes corresponding to the same dose, which would be printed onto the edible substrate using the developed HC-loaded inks in single dose printing.

For the data matrix printing, the software indicated the number of layers needed and adjusted the data matrix code size to obtain a specific dose. These options, in combination with the accuracy of inkjet printing, can obtain ODFs with a personalized dose and a data matrix code which can be read easily with a smartphone. The web-based software prototype can be complemented with a smartphone application that captures the printed code by the camera integrated in the device, providing access to the information contained within the data matrix code (Figure 5). The data matrix codes can only be read by the specialized application, ensuring that access to sensitive information, like patient data, is restricted to authorized personnel. This remains in line with patient confidentiality and prevents inadequate use of healthcare information. Moreover, in this way data matrix codes can be securely tracked, providing a safe approach for drug traceability.

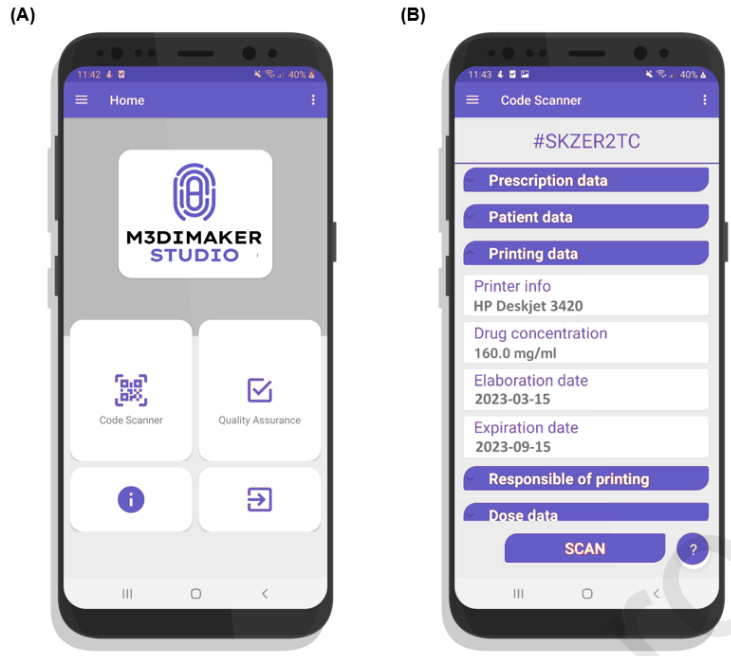

Figure 5. Diagram of the user interface process in M3DIMAKER Studio™: (A) Selection of the Code Scanner and (B) Code Scanner mode in which the code printed on the film is read and information related to the dose, the patient, the printer used, and many more are given.

3.3 Inkjet printing of hydrocortisone films

Printing was carried out with the HP Deskjet 3420 printer and on a 0.3 mm thickness potato starch paper, due to the versatility and consistency showed in the preliminary tests. All inks showed in Table 1 obtained good printability results, apart from the inks containing Soluplus® (not printable).

Data matrix codes of the same size were generated using M3DIMAKER Studio™ and were printed using the different pharma-inks (Figure 6A). To highlight the possibility of carrying out a multiple printing approach, data matrix codes with different sizes were generated by the software and printed also (Figure 6B). During the printing process, films with up to 3 layers of ink and good resolution were obtained using a data matrix pattern with relevant encoded information that can be read with any smartphone (Figure 5). A total of 10 minutes was elapsed between printing each of the layers to ensure complete absorption of the pharma-ink.

(A)

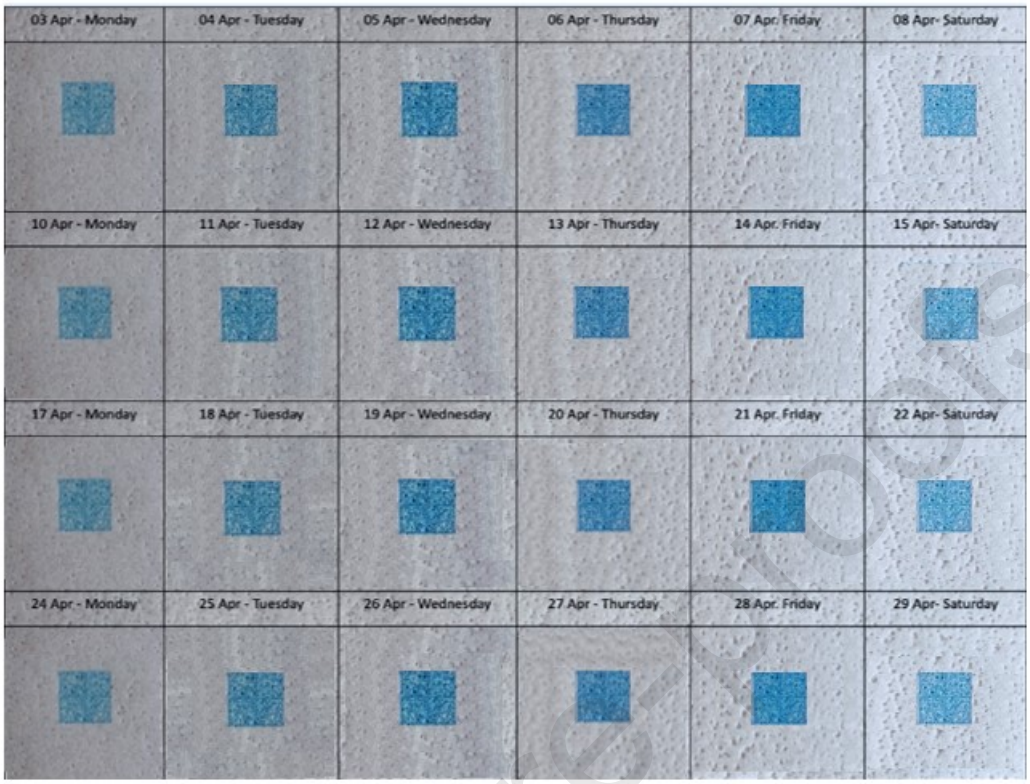

1

2

(B)

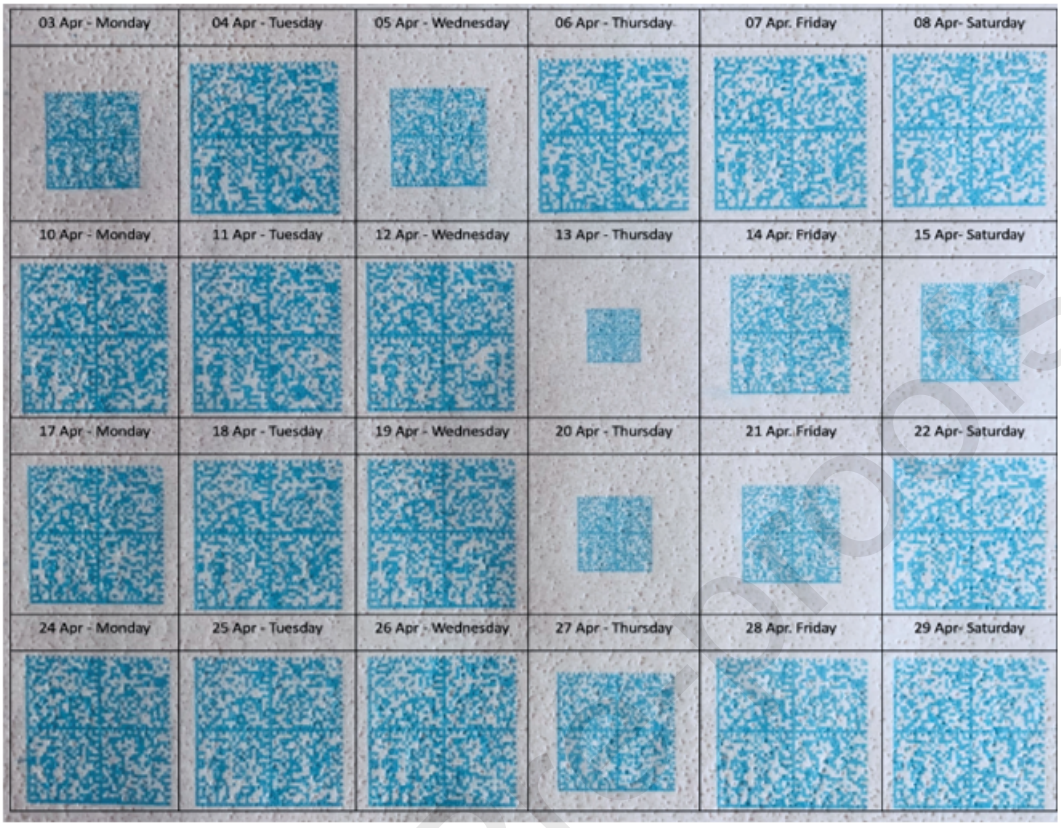

Figure 6. Image of data matrix codes containing HC printed on the potato starch edible substrate: a) Single dose printing (2 cm^2); b) Multiple dose printing. Film areas range from 10.24 cm^2 to 2 cm^2.

Multiple dose printing is an interesting approach where treatment dosage varies over time (same day or different days) and continuous dose adjustments are necessary, such as HC for adrenal insufficiency in children. It is also important in hormone replacement therapy to mimic the natural production pattern of the hormone cortisol(Chan and Debono, 2010). Plasma cortisol levels change throughout the day, reaching the maximum concentration peak in the morning and the minimum concentration at night. With the multiple dose printing option provided by M3DIMAKER Studio™, different doses can be printed that mimic the circadian rhythm of cortisol, improving the efficacy of the treatment. In addition, corticosteroids (e.g. prednisone and dexamethasone) are also prescribed for the control of certain inflammatory processes and for supressing the immune system response that may cause inhibition of the hypothalamic–pituitary–adrenal axis(Pelewicz and Miśkiewicz, 2021). Instant reduction or cessation of exogenous corticosteroids may cause symptoms of adrenal insufficiency or lead to adrenal crisis. Therefore, the daily dose of corticosteroids is reduced so that the natural production of cortisol is restored in the patient. The tapering of the corticosteroid dose can be easily prepared with the multiple dose printing approach, allowing the printing of doses adjusted to the reduction scheme, saving cost and time whilst increasing the safety of the treatment due to the encoded information.

3.4 Drug content in the printed films

To obtain preliminary information and to optimize the data matrix code generation, solid squares with a constant area of 2 cm^2 were printed using PG:H_2O 60:40 v/v and PG:H_2O 30:70 v/v base inks. Up to 3 layers were printed. The HC was quantified with the HPLC method mentioned in Section 2.6. As shown in Figure 7, the amount of drug deposited was very low, reaching a maximum of ~103 µg of HC after 3 layers. As the number of layers increased, so did the amount of deposited HC. A maximum deposition of 103 µg of HC was obtained using the PG:H_2O (60:40 v/v) + HC:β-CD (1:3 w/w) ink. The amount of HC deposited on the film was higher for the 60:40 ratio ink compared to the 30:70 ink. These findings are related to the results obtained from the solubility of the drug in the different inks. In addition, inclusion complexation with β-CD increased the amount of HC deposited compared to both 60:40 and 30:70 inks.

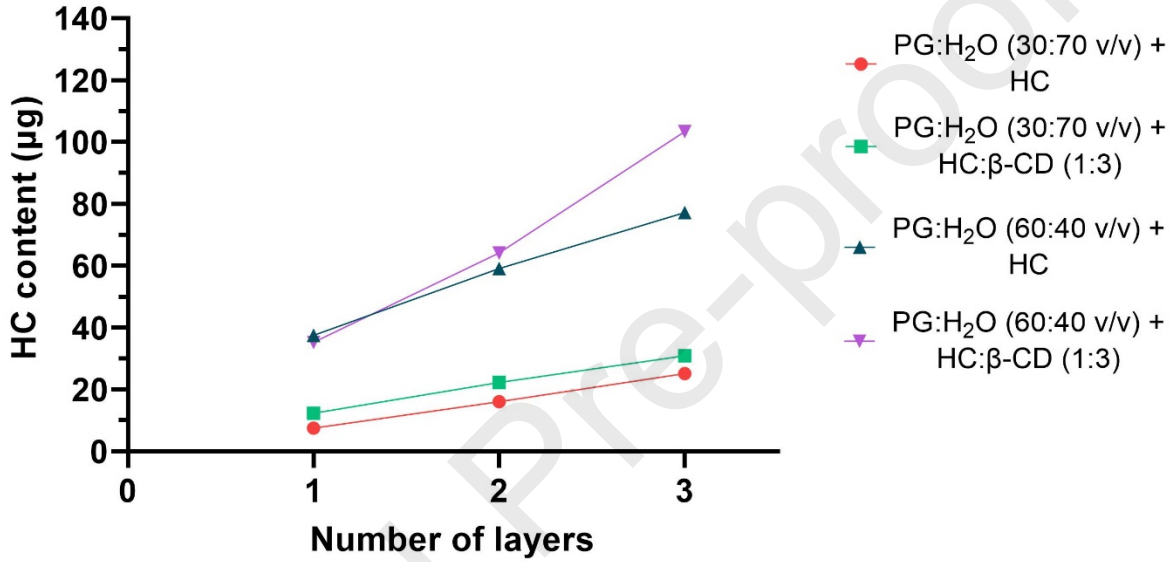

Figure 7. Graphical representation that compares the amount of HC (µg) deposited on the solid square films with an area of 2 cm^2 as a function of the number of printed layers and the use of different inks.

Once the amount of printed HC in squares with an area of 2 cm^2 was quantified, the data matrix codes were printed with the "single dose printing" option in the developed software (Figure 8).

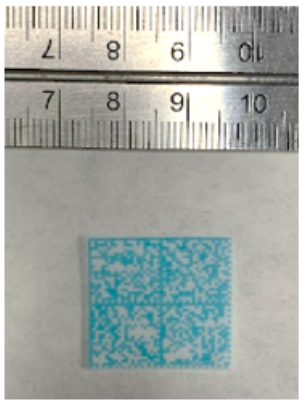

Figure 8. Image of the developed and printed data matrix film using the single dose printing option. Scale is in cm.

The amount of printed HC was determined following the same HPLC method. In view of the results obtained in Figure 9, the amount of deposited HC decreased slightly compared to the solid square films due to the empty space to codify the information.

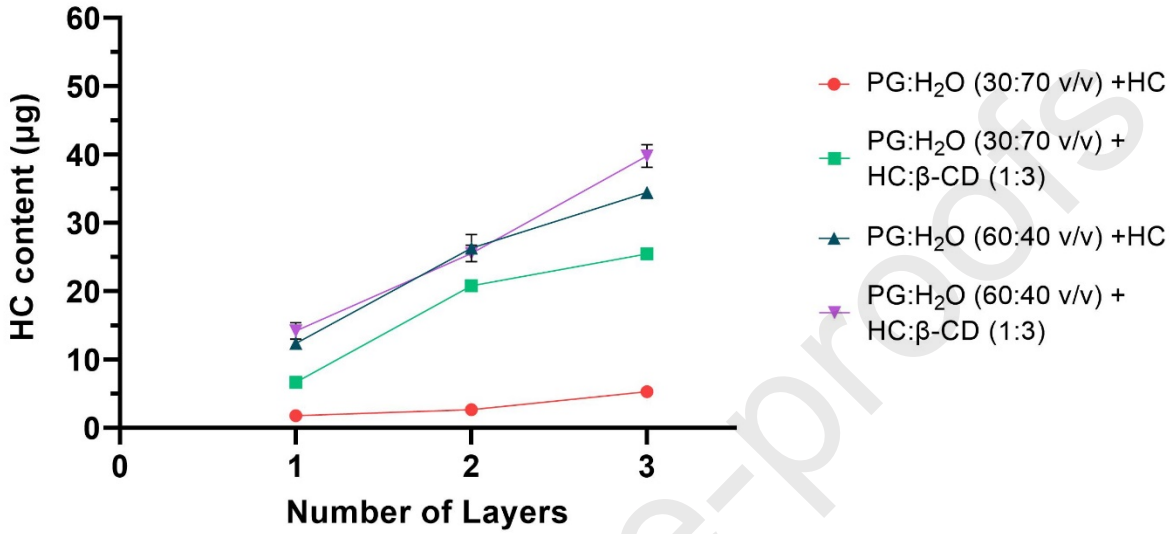

Figure 9. Graphical representation that compares the amount of HC (µg) deposited on the data matrix code films, depending on the number of printed layers and the use of different inks.

The maximum printed HC in the printed data matrix examples was ~40 µg with PG:H_2O (60:40 v/v) + HC:β-CD (1:3 w/w) ink. The reason for this being the presence of ink free areas within the data matrix code in comparison to the solid square. The obtained results showed the same trend as those obtained with the square. The amount of HC deposited on films printed with 60:40 inks was higher than with the 30:70 inks. For both the solid square films and the data matrix code films, the highest amounts of HC were obtained with the inks with the highest proportion of PG. Therefore, it can be observed that a higher proportion of organic solvent as well as the use of cyclodextrins caused an increase in the solubility of the HC within the ink, increasing the drug content deposited on the substrate. Conversely, the amount of HC deposited with the cyclodextrin-containing inks was not as high as expected from looking at the results in Figure 8. In the case of the 30:70 ratio ink, there were differences between the ink with and without cyclodextrins in terms of the amount of drug printed in data matrix pattern. However, there were no differences between the ink with and without cyclodextrins in the case of 60:40 ratio ink. The HC deposited was slightly higher in the third layer with the ink containing cyclodextrins.

For the first time, a data matrix code generator software specifically made for the healthcare sector was successfully combined with inkjet printing to produce films containing HC. Scaled data matrix codes which encoded relevant information were generated using M3DIMAKER Studio™ software and personalized HC films were prepared by varying the number of printed layers. The data matrix codes can be easily read using a smartphone application, improving the traceability and safety of the treatment. The printed HC doses using a desktop printer were far from the recommended oral doses (10 - 30 mg divided in three or four administrations) since 103 µg and 40 µg were deposited on solid square and data matrix films, respectively. A dose

closer to the target could be accomplished with a higher concentration pharma-ink or specialised pharmaceutical inkjet printer able to print several layers in an easier manner. No pharmaceutical inkjet printers are available on the market and desktop or conventional printers are currently adapted to assess pharmaceutical applications. Therefore, there is a need for specialised pharmaceutical inkjet printers that can overcome the main limitations of inkjet printing (e.g. inconsistency, paper jam), offering better printing performance and avoiding variability in the drug deposition.

3.5 Disintegration testing

Since, there are no official guidelines available for determining disintegration time of fast disintegrating oral films, one of the most widely used methods in the literature, the slide frame method, was adapted for this test (Irfan et al., 2016; Speer et al., 2018). The result was expressed as the average time alongside standard deviation. The assay showed a fast disintegration of the film, only 5.3 ± 0.7 sec, leading to a fast disintegration in the mouth and hence, improved absorption and quicker onset of drug action. According to this disintegration time, rapid dissolution of the film is expected, and all the drug is released in a matter of seconds. As the ODF is dissolved in the saliva and is in contact with the taste buds, taste acceptability is an important factor to consider, especially in terms of paediatric treatment. Since hydrocortisone is a bitter drug, it would benefit from taste masking approaches for ODFs. The use of cyclodextrins has been studied extensively for its taste masking capabilities (Adamkiewicz and Szeleszczuk, 2023), and could be a potential avenue for the taste masking of hydrocortisone for ODFs. In this study, the highest printed dose was obtained with PG:H_2O (60:40 v/v) + HC:β-CD (1:3 w/w) ink. This pharma-ink was based on drug-complexation using cyclodextrins to increase the drug loading within the ODF. Due to acceptability issues in paediatric patients and the bitter taste of hydrocortisone, this pharma-ink may be beneficial for paediatrics because the complexation with cyclodextrins can also mask the bitter taste of the drug. As a result, it could be implemented in clinical practice to improve not only the treatment performance, but also the acceptability.

4. Conclusions

A software specifically designed for the healthcare sector was successfully implemented in combination with inkjet printing technology to prepare data-enriched edible films containing a potent drug, hydrocortisone. The films were printed and encoded relevant information regarding the dosage form, treatment, and patient details. The amount of deposited drug increased with the number of printed layers; therefore, it is possible to prepare personalized data-enriched edible films by modifying the number of printed layers. Moreover, it was demonstrated that it is possible to print different sizes of data matrix codes increasing the dose selection options. With the multiple dose printing approach, time, and cost savings alongside the safety of the treatment would be increased by encoding information that is easily readable by the patients using an application in their smartphones. With the application, healthcare personnel can scan the data matrix code at any time, thereby improving medicine traceability.

Drug solubility studies carried out in different pharma-inks indicated that the HC concentrations obtained were low. It was observed that the higher proportion of PG in the formulation of the pharma-inks caused an increase in the solubility of HC and, simultaneously, acted as a humectant agent and viscosity and surface tension modifier. It can be stated that there was an improvement in solubility for both inclusion complexes with β-cyclodextrin or

micelles with Soluplus®. The formation of inclusion complexes with cyclodextrins increased the solubility of the drug and, therefore, the amount deposited in each layer. In addition, the complexation of hydrocortisone with cyclodextrins can also mask its bitter taste, improving its acceptability and adherence. However, the findings of this study indicated that not all pharma-inks were printable, even with Z values within the accepted range (1 - 10), suggesting that the Z value may not be the best parameter to predict ink printability, as already found in a previous inkjet printability ML study.

This work demonstrates the ever-growing potential of inkjet printing and opens the possibility of using it to obtain flexible doses of drugs that are prescribed at low doses in clinical practice. In addition, the preliminary information obtained in this study allows the optimization of the software, to achieve a precise scalation of codes that will provide personalized doses. The development of a code generator software oriented to medical use provides an additional, innovative, and revolutionary advantage: the incorporation of data matrix codes, easily read with a simple smartphone, to increase the safety, traceability, and efficacy of prescribed treatments.

Acknowledgments: The work was partially supported by MCIN [PID 2020-113881RB-I00/AEI/10.13039/501100011033], Spain, Xunta de Galicia [ED431C 2020/17], and FEDER. LRP acknowledges the predoctoral fellowship [FPU20/01245] provided by the Ministerio de Universidades [Formación de Profesorado Universitario (FPU 2020)]. PCS acknowledges the Predoctoral Fellowship [Programa de axudas á etapa predoutoral, grant number ED481A 2023] from Xunta de Galicia (Consellería de Cultura, Educación, Formación Profesional e Universidades).

References

Abdel Jalil, M., Abdullah, N., Alsous, M., Abu-Hammour, K., 2021. Population Pharmacokinetic Studies of Digoxin in Adult Patients: A Systematic Review, in: Eur J Drug Metab Pharmacokinet. France, pp. 325–342. https://doi.org/10.1007/s13318-021-00672-6

Adamkiewicz, L., Szeleszczuk, Ł., 2023. Review of Applications of Cyclodextrins as Taste-Masking Excipients for Pharmaceutical Purposes. Molecules 28, 6964. https://doi.org/10.3390/molecules28196964

Alomari, M., Vuddanda, P.R., Trenfield, S.J., Dodoo, C.C., Velaga, S., Basit, A.W., Gaisford, S., 2018. Printing T3 and T4 oral drug combinations as a novel strategy for hypothyroidism. Int J Pharm 549, 363–369. https://doi.org/https://doi.org/10.1016/j.ijpharm.2018.07.062

Arshad, M.S., Shahzad, A., Abbas, N., AlAsiri, A., Hussain, A., Kucuk, I., Chang, M.W., Bukhari, N.I., Ahmad, Z., 2020. Preparation and characterization of indomethacin loaded films by piezoelectric inkjet printing: a personalized medication approach. Pharm Dev Technol 25, 197–205. https://doi.org/10.1080/10837450.2019.1684520

Azizi Machekposhti, S., Mohaved, S., Narayan, R.J., 2019. Inkjet dispensing technologies: recent advances for novel drug discovery. Expert Opin Drug Discov 14, 101–113. https://doi.org/10.1080/17460441.2019.1567489

Boehm, R.D., Miller, P.R., Daniels, J., Stafslien, S., Narayan, R.J., 2014. Inkjet printing for pharmaceutical applications. Materials Today 17, 247–252. https://doi.org/10.1016/j.mattod.2014.04.027

Boehm, R.D., Miller, P.R., Schell, W.A., Perfect, J.R., Narayan, R.J., 2013. Inkjet Printing of Amphotericin B onto Biodegradable Microneedles Using Piezoelectric Inkjet Printing. JOM 65, 525–533. https://doi.org/10.1007/s11837-013-0574-7

Carou-Senra, P., Ong, J.J., Castro, B.M., Seoane-Viaño, I., Rodríguez-Pombo, L., Cabalar, P., Alvarez-Lorenzo, C., Basit, A.W., Pérez, G., Goyanes, A., 2023. Predicting pharmaceutical inkjet printing outcomes using machine learning. Int J Pharm X 5, 100181. https://doi.org/10.1016/j.ijpx.2023.100181

Chan, S., Debono, M., 2010. Replication of cortisol circadian rhythm: new advances in hydrocortisone replacement therapy. Ther Adv Endocrinol Metab 1, 129–138. https://doi.org/10.1177/2042018810380214

Chao, M., Genina, N., Beer, N., Kälvemark Sporrong, S., 2022. Data-enriched edible pharmaceuticals (DEEPs): Patients' preferences, perceptions, and acceptability of new dosage forms and their digital aspects – An interview study. Exploratory Research in Clinical and Social Pharmacy 6, 100141. https://doi.org/10.1016/j.rcsop.2022.100141

Chao, M., Öblom, H., Cornett, C., Bøtker, J., Rantanen, J., Sporrong, S.K., Genina, N., 2021. Data-Enriched Edible Pharmaceuticals (DEEP) with Bespoke Design, Dose and Drug Release. Pharmaceutics 13, 1866. https://doi.org/10.3390/pharmaceutics13111866

Chou, W.-H., Gamboa, A., Morales, J.O., 2021. Inkjet printing of small molecules, biologics, and nanoparticles. Int J Pharm 600, 120462. https://doi.org/10.1016/j.ijpharm.2021.120462

Cui, M., Pan, H., Su, Y., Fang, D., Qiao, S., Ding, P., Pan, W., 2021. Opportunities and challenges of three-dimensional printing technology in pharmaceutical formulation development. Acta Pharm Sin B 11, 2488–2504. https://doi.org/10.1016/j.apsb.2021.03.015

Daly, R., Harrington, T.S., Martin, G.D., Hutchings, I.M., 2015. Inkjet printing for pharmaceutics – A review of research and manufacturing. Int J Pharm 494, 554–567. https://doi.org/10.1016/j.ijpharm.2015.03.017

Derby, B., 2015. Additive Manufacture of Ceramics Components by Inkjet Printing. Engineering 1, 113–123. https://doi.org/10.15302/J-ENG-2015014

Alkindi Product information. European Medicines Agency (EMA), 2023. [WWW Document], n.d. URL https://www.ema.europa.eu/en/medicines/human/EPAR/alkindi (accessed 11.21.23).

Efmody Product information. European Medicines Agency (EMA), 2023. [WWW Document], n.d. URL https://www.ema.europa.eu/en/medicines/human/EPAR/efmody#:~:text=Efmody%20is%20available%20as%20modified,15%20to%2025%20mg%20daily. (accessed 11.21.23).

Plenadren Product information. European Medicines Agency (EMA) [WWW Document], n.d. URL https://www.ema.europa.eu/en/medicines/human/EPAR/plenadren (accessed 11.20.23).

Edinger, M., Bar-Shalom, D., Sandler, N., Rantanen, J., Genina, N., 2018. QR encoded smart oral dosage forms by inkjet printing. Int J Pharm 536, 138–145. https://doi.org/https://doi.org/10.1016/j.ijpharm.2017.11.052

El-Maouche, D., Arlt, W., Merke, D.P., 2017. Congenital adrenal hyperplasia. Lancet 390, 2194–2210. https://doi.org/10.1016/s0140-6736(17)31431-9

Genina, N., Fors, D., Palo, M., Peltonen, J., Sandler, N., 2013. Behavior of printable formulations of loperamide and caffeine on different substrates—Effect of print density in inkjet printing. Int J Pharm 453, 488–497. https://doi.org/10.1016/j.ijpharm.2013.06.003

Genina, N., Fors, D., Vakili, H., Ihalainen, P., Pohjala, L., Ehlers, H., Kassamakov, I., Haeggström, E., Vuorela, P., Peltonen, J., Sandler, N., 2012. Tailoring controlled-release oral dosage forms by combining inkjet and flexographic printing techniques. European Journal of Pharmaceutical Sciences 47, 615–623. https://doi.org/10.1016/j.ejps.2012.07.020

Handa, M., Afzal, O., Beg, S., Nashik Sanap, S., Kaundal, R.K., Verma, R.K., Mishra, A., Shukla, R., 2023. Harnessing personalized tailored medicines to digital-based data-enriched edible pharmaceuticals. Drug Discov Today 28, 103555. https://doi.org/10.1016/j.drudis.2023.103555

Hoffmann, E.M., Breitenbach, A., Breitkreutz, J., 2011. Advances in orodispersible films for drug delivery. Expert Opin Drug Deliv 8, 299–316. https://doi.org/10.1517/17425247.2011.553217

Husebye, E.S., Pearce, S.H., Krone, N.P., Kämpe, O., 2021. Adrenal insufficiency. Lancet 397, 613–629. https://doi.org/10.1016/s0140-6736(21)00136-7

Hydrocortisone | C21H30O5 | CID 5754 - PubChem [WWW Document], n.d. URL https://pubchem.ncbi.nlm.nih.gov/compound/Hydrocortisone (accessed 11.21.23).

Irfan, M., Rabel, S., Bukhtar, Q., Qadir, M.I., Jabeen, F., Khan, A., 2016. Orally disintegrating films: A modern expansion in drug delivery system. Saudi Pharmaceutical Journal 24, 537–546. https://doi.org/10.1016/j.jsps.2015.02.024

Jang, D., Kim, D., Moon, J., 2009. Influence of Fluid Physical Properties on Ink-Jet Printability. Langmuir 25, 2629–2635. https://doi.org/10.1021/la900059m

Khan, D., Kirby, D., Bryson, S., Shah, M., Rahman Mohammed, A., 2022. Paediatric specific dosage forms: Patient and formulation considerations. Int J Pharm 616, 121501. https://doi.org/10.1016/j.ijpharm.2022.121501

Kiefer, O., Fischer, B., Breitkreutz, J., 2021. Fundamental Investigations into Metoprolol Tartrate Deposition on Orodispersible Films by Inkjet Printing for Individualised Drug Dosing. Pharmaceutics 13, 247. https://doi.org/10.3390/pharmaceutics13020247

Liu, Y., Derby, B., 2019. Experimental study of the parameters for stable drop-on-demand inkjet performance. Physics of Fluids 31. https://doi.org/10.1063/1.5085868

Meléndez, P.A., Kane, K.M., Ashvar, C.S., Albrecht, M., Smith, P.A., 2008. Thermal Inkjet Application in the Preparation of Oral Dosage Forms: Dispensing of Prednisolone Solutions and Polymorphic Characterization by Solid-State Spectroscopic Techniques. J Pharm Sci 97, 2619–2636. https://doi.org/10.1002/jps.21189

Mohd Azmi, N.A.S., Juliana, N., Azmani, S., Mohd Effendy, N., Abu, I.F., Mohd Fahmi Teng, N.I., Das, S., 2021. Cortisol on Circadian Rhythm and Its Effect on Cardiovascular System. Int J Environ Res Public Health 18. https://doi.org/10.3390/ijerph18020676

Nadagouda, M.N., Rastogi, V., Ginn, M., 2020. A review on 3D printing techniques for medical applications. Curr Opin Chem Eng 28, 152–157. https://doi.org/10.1016/j.coche.2020.05.007

Nallan, H.C., Sadie, J.A., Kitsomboonloha, R., Volkman, S.K., Subramanian, V., 2014. Systematic Design of Jettable Nanoparticle-Based Inkjet Inks: Rheology, Acoustics, and Jettability. Langmuir 30, 13470–13477. https://doi.org/10.1021/la502903y

Nisticò, D., Bossini, B., Benvenuto, S., Pellegrin, M.C., Tornese, G., 2022. Pediatric Adrenal Insufficiency: Challenges and Solutions. Ther Clin Risk Manag 18, 47–60. https://doi.org/10.2147/tcrm.s294065

Nørfeldt, L., Bøtker, J., Edinger, M., Genina, N., Rantanen, J., 2019. Cryptopharmaceuticals: Increasing the Safety of Medication by a Blockchain of Pharmaceutical Products. J Pharm Sci 108, 2838–2841. https://doi.org/10.1016/j.xphs.2019.04.025

Öblom, H., Cornett, C., Bøtker, J., Frokjaer, S., Hansen, H., Rades, T., Rantanen, J., Genina, N., 2020. Data-enriched edible pharmaceuticals (DEEP) of medical cannabis by inkjet printing. Int J Pharm 589, 119866. https://doi.org/10.1016/j.ijpharm.2020.119866

Pelewicz, K., Miśkiewicz, P., 2021. Glucocorticoid Withdrawal—An Overview on When and How to Diagnose Adrenal Insufficiency in Clinical Practice. Diagnostics 11, 728. https://doi.org/10.3390/diagnostics11040728

Pollard, T.D., Bonetti, M., Day, A., Gaisford, S., Orlu, M., Basit, A.W., Murdan, S., Goyanes, A., 2022. Printing Drugs onto Nails for Effective Treatment of Onychomycosis. Pharmaceutics 14, 448. https://doi.org/10.3390/pharmaceutics14020448

Pollard, T.D., Seoane-Viaño, I., Ong, J.J., Januskaite, P., Awwad, S., Orlu, M., Bande, M.F., Basit, A.W., Goyanes, A., 2023. Inkjet drug printing onto contact lenses: Deposition optimisation and non-destructive dose verification. Int J Pharm X 5, 100150. https://doi.org/10.1016/j.ijpx.2022.100150

Raijada, D., Wac, K., Greisen, E., Rantanen, J., Genina, N., 2021. Integration of personalized drug delivery systems into digital health. Adv Drug Deliv Rev 176, 113857. https://doi.org/10.1016/j.addr.2021.113857

Rodriguez-Aller, M., Guillarme, D., Veuthey, J.-L., Gurny, R., 2015. Strategies for formulating and delivering poorly water-soluble drugs. J Drug Deliv Sci Technol 30, 342–351. https://doi.org/10.1016/j.jddst.2015.05.009

Sandler, N., Määttänen, A., Ihalainen, P., Kronberg, L., Meierjohann, A., Viitala, T., Peltonen, J., 2011. Inkjet printing of drug substances and use of porous substrates-towards individualized dosing. J Pharm Sci 100, 3386–3395. https://doi.org/10.1002/jps.22526

Scoutaris, N., Chai, F., Maurel, B., Sobocinski, J., Zhao, M., Moffat, J.G., Craig, D.Q., Martel, B., Blanchemain, N., Douroumis, D., 2016. Development and Biological Evaluation of Inkjet Printed Drug Coatings on Intravascular Stent. Mol Pharm 13, 125–133. https://doi.org/10.1021/acs.molpharmaceut.5b00570

Seoane-Viaño, I., Trenfield, S.J., Basit, A.W., Goyanes, A., 2021. Translating 3D printed pharmaceuticals: From hype to real-world clinical applications. Adv Drug Deliv Rev 174, 553–575. https://doi.org/10.1016/j.addr.2021.05.003

Singh, M., Haverinen, H.M., Dhagat, P., Jabbour, G.E., 2010. Inkjet Printing—Process and Its Applications. Advanced Materials 22, 673–685. https://doi.org/10.1002/adma.200901141

Speer, I., Steiner, D., Thabet, Y., Breitkreutz, J., Kwade, A., 2018. Comparative study on disintegration methods for oral film preparations. European Journal of Pharmaceutics and Biopharmaceutics 132, 50–61. https://doi.org/10.1016/j.ejpb.2018.09.005

Ebnesajjad S., 2009. Surface Tension and Its Measurement, in: Adhesives Technology Handbook. Elsevier, pp. 21–36. https://doi.org/10.1016/B978-0-8155-1533-3.50005-0

Turner, R.M., Park, B.K., Pirmohamed, M., 2015. Parsing interindividual drug variability: an emerging role for systems pharmacology. Wiley Interdiscip Rev Syst Biol Med 7, 221–241. https://doi.org/10.1002/wsbm.1302

Varan, C., Wickström, H., Sandler, N., Aktaş, Y., Bilensoy, E., 2017. Inkjet printing of antiviral PCL nanoparticles and anticancer cyclodextrin inclusion complexes on bioadhesive film for cervical administration. Int J Pharm 531, 701–713. https://doi.org/10.1016/j.ijpharm.2017.04.036

Vaz, V.M., Kumar, L., 2021. 3D Printing as a Promising Tool in Personalized Medicine. AAPS PharmSciTech 22, 49. https://doi.org/10.1208/s12249-020-01905-8

Vuddanda, P.R., Alomari, M., Dodoo, C.C., Trenfield, S.J., Velaga, S., Basit, A.W., Gaisford, S., 2018. Personalisation of warfarin therapy using thermal ink-jet printing. Eur J Pharm Sci 117, 80–87. https://doi.org/10.1016/j.ejps.2018.02.002

Waasdorp, R., van den Heuvel, O., Versluis, F., Hajee, B., Ghatkesar, M.K., 2018. Accessing individual 75-micron diameter nozzles of a desktop inkjet printer to dispense picoliter droplets on demand. RSC Adv 8, 14765–14774. https://doi.org/10.1039/C8RA00756J

Watson, C.J., Whitledge, J.D., Siani, A.M., Burns, M.M., 2021. Pharmaceutical Compounding: a History, Regulatory Overview, and Systematic Review of Compounding Errors. Journal of Medical Toxicology 17, 197–217. https://doi.org/10.1007/s13181-020-00814-3

Wening, K., Breitkreutz, J., 2011. Oral drug delivery in personalized medicine: unmet needs and novel approaches. Int J Pharm 404, 1–9. https://doi.org/10.1016/j.ijpharm.2010.11.001

Whitaker, M.J., Spielmann, S., Digweed, D., Huatan, H., Eckland, D., Johnson, T.N., Tucker, G., Krude, H., Blankenstein, O., Ross, R.J., 2015. Development and testing in healthy adults of oral hydrocortisone granules with taste masking for the treatment of neonates and infants with adrenal insufficiency. J Clin Endocrinol Metab 100, 1681–1688. https://doi.org/10.1210/JC.2014-4060

Wickström, H., Palo, M., Rijckaert, K., Kolakovic, R., Nyman, J.O., Määttänen, A., Ihalainen, P., Peltonen, J., Genina, N., de Beer, T., Löbmann, K., Rades, T., Sandler, N., 2015. Improvement of dissolution rate of indomethacin by inkjet printing. European Journal of Pharmaceutical Sciences 75, 91–100. https://doi.org/10.1016/j.ejps.2015.03.009

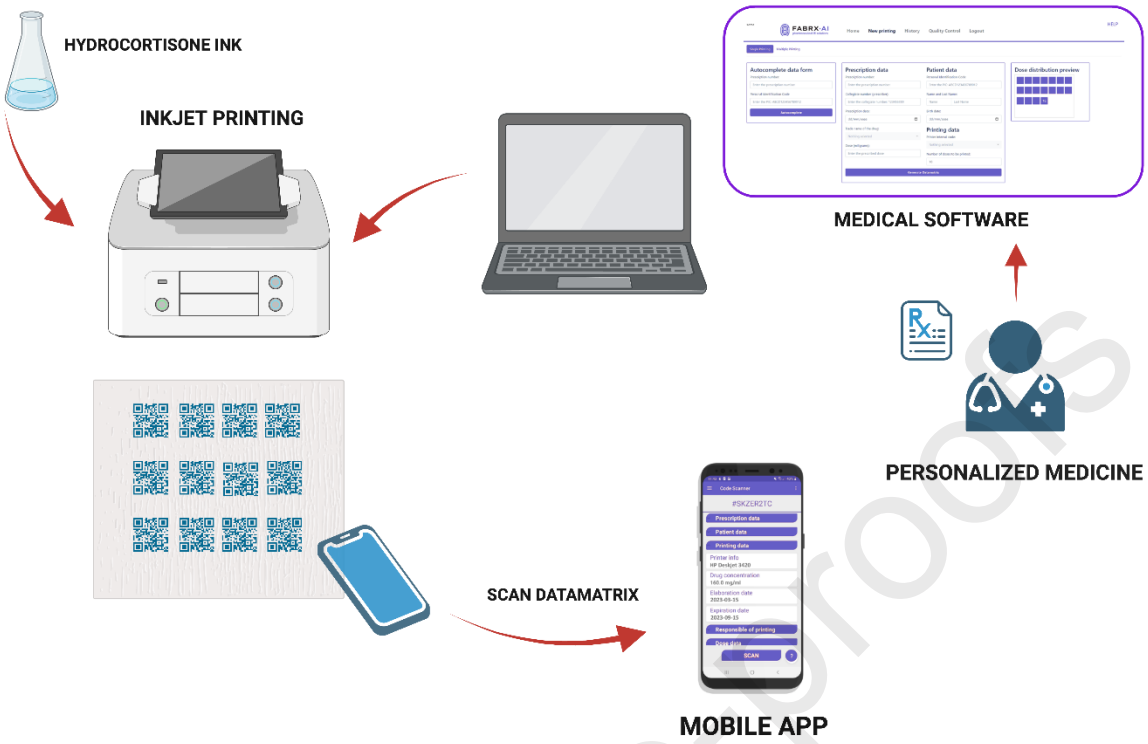

Declaration of interests

☐ The authors declare that they have no known competing financial interests or personal relationships that could have appeared to influence the work reported in this paper.

☒ The authors declare the following financial interests/personal relationships which may be considered as potential competing interests:

Alvaro Goyanes reports a relationship with FABRX Ltd. that includes: employment and equity or stocks. Abdul Basit reports a relationship with FABRX Ltd. that includes:. Carlos Rial reports a relationship with FABRX AI Ltd. that includes: employment. Corresponding author part of the editorial board in International Journal of Pharmaceutics - A.B. If there are other authors, they declare that they have no known competing financial interests or personal relationships that could have appeared to influence the work reported in this paper.